Pergamon

Int. J. Solids Structures Vol. 35, Nos 26–27, pp. 3573–3593, 1998

0020–7683/98 $19.00 + .00

PII: S0020–7683(98)00023–7

ON THE GENERAL TREATMENT OF MULTIPLE INCLUSIONS IN ANTIPLANE ELASTOSTATICS

C. K. CHAO* and C. W. YOUNG
Department of Mechanical Engineering, National Taiwan University of Science and Technology, Taipei, Taiwan, 106, R.O.C.

(*Received* 9 *July* 1997; *in revised form* 5 *January* 1998)

Abstract—This article provides an explicit general solution of an infinitely extended plate containing any number of circular inclusions under antiplane deformation. The derived solution of the present heterogeneous problem associated with multiple inclusions is obtained in terms of the corresponding homogeneous solution by a simple algebraic substitution. This is accomplished by the technique of analytical continuation and the method of successive approximations. A rapidly convergent series solution either in the matrix or in the inclusions, which is expressed in terms of an explicit general term involving the complex potential of the corresponding homogeneous problem, is derived in an elegant form. The present derived solution can also be applied to the inclusion problem with straight boundaries. Numerical examples of three circular inclusions embedded in an infinite matrix, in a half-plane matrix, and in a strip are discussed in detail and displayed in graphic form. Interaction of a crack with multiple circular inclusions is also considered. © 1998 Elsevier Science Ltd. All rights reserved.

1. INTRODUCTION

The problem of interacting cracks near a single inclusion has been investigated by many researchers. One of the most powerful methods in solving this problem is based upon the method of analytical continuation which allows us to easily deal with interface continuity conditions along the common boundary between dissimilar media. Following this approach, the derived solution associated with the heterogeneous problem can be obtained in terms of the corresponding homogeneous solution by a simple algebraic substitution. By applying the existing solution for dislocations in the homogeneous problem, a system of singular integral equations for the related crack problems is then obtained in a way that the relevant boundary conditions along the crack border should be satisfied. As to the problem with multiple inclusions, the above-mentioned methodology, however, cannot be directly used to deal with two or more separate interfaces that a closed-form solution is difficult to achieve. The particular problem of two circular inclusions under longitudinal shear loading has been solved by Goree and Wilson (1967) using a mapping function with the aid of a bilinear transformation. Sendeckyj (1971) resolved the same problem by applying a successive approximation method. The corresponding problem of two traction-free holes has been considered by Steif (1989) using a series solution. Zimmerman (1988) further discussed the stress concentration around a pair of circular holes in a hydrostatically stressed elastic sheet solved by Kienzler and Duan (1987) who derived a simple formula to calculate the distribution of hoop stresses by employing the Fourier series expansion. Based on the use of complex potentials and the Laurent series expansion method, Gong (1995) solved the antiplane problem with multiple circular inclusions. Elastic fields of interacting inhomogeneities were studied by Horii and Nemat-Nasser (1985) using the method of pseudo-tractions. Recently, Chao *et al.* (1997) investigated the problem of interacting circular inclusions in plane thermoelasticity by the use of Laurent series expansion. All the aforementioned approaches, however, are cumbersome due to the necessity of solving the large system of equations resulting from interfacial boundary conditions. Besides, those approaches are unable to deal with the interaction between cracks (or singularities) and multiple inclusions. To overcome the shortcoming of the above-mentioned methods, the technique of

* Author to whom correspondence should be addressed. E-mail: ckchao@mail.ntust.edu.tw.

analytical continuation and the method of successive approximations are exploited here to solve the multiple inclusion problem which permit us to express the solution as a rapidly convergent series. Since the complex potential of the corresponding homogeneous problem is involved in a series solution, studies on the interaction of cracks or singularities with multiple inclusions can be easily achieved by solving a system of singular integral equations. Note that, the present proposed method can be applied not only for the inclusion problem with circular boundaries but also for the inclusion problem with straight boundaries.

In this paper, our purpose is to derive an explicit general solution of the antiplane problem containing an arbitrary number of inclusions with circular or straight boundaries. The derived closed form solution for the problem containing multiple inclusions is expressed in terms of the corresponding homogeneous solution. This merely implies that the solution associated with the heterogeneous problem containing any number of inclusions can be determined immediately once the problem when the matrix material occupies the whole space and is subjected to the same loading (singularities) is solved. This was termed "heterogenization" by Honein *et al.* (1992a). By introducing the dislocation functions associated with the homogeneous problem, the mode-III stress intensity factor for the heterogeneous problem can be directly obtained by solving the singular integral equations with a logarithmic singular kernel. Numerical examples of three circular inclusions interacting with an arbitrarily located crack are given to illustrate the use of the present approach. The results presented here may assist in studies of crack interaction with a non-uniform distribution of fibers in a composite under antiplane deformation.

2. INTERACTING CIRCULAR INCLUSIONS

Consider the antiplane problem of an arbitrary number of circular inclusions embedded in an infinitely extended solid. Each circular inclusion has different elastic constants from those of the matrix. Let the regions S_j be occupied by an array of circular inclusions centered with z_j, of arbitrary radii a_j and of different shear moduli μ_j, which are perfectly bonded to the region S occupied by the matrix of infinite extent and of shear modulus μ (see Fig. 1).

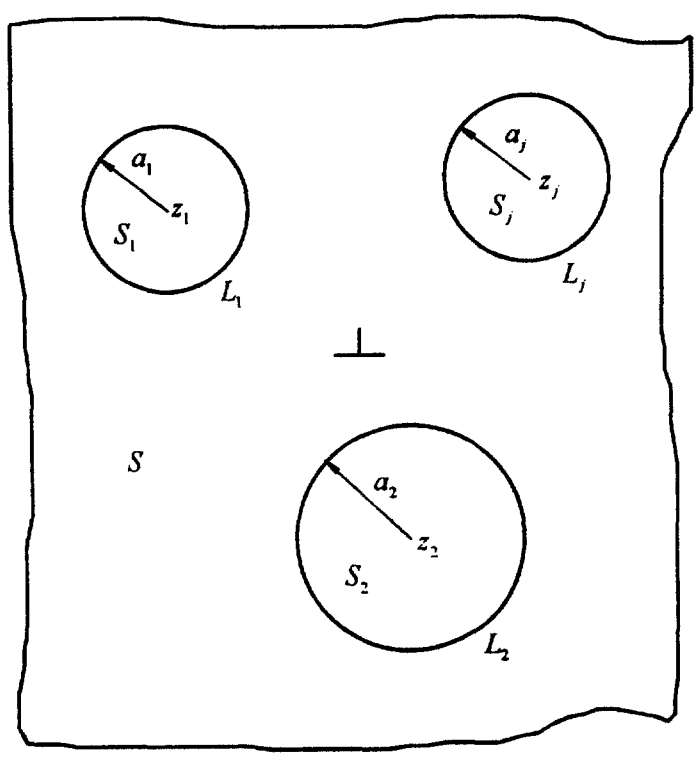

Fig. 1. Multiple circular inclusions perfectly bonded to an infinite matrix.

Our purpose is to find the stress potentials $\phi(z)$ and $\phi^{(j)}(z)$ where all the singularities (loads) are in the matrix. Under antiplane deformations, the displacement u, resultant force p and shear stresses σ_{xt}, σ_{yt} in x- and y-directions, respectively, can be represented in terms of the stress potential as (Muskhelishvili, 1953)

$$\omega = 2\,\mathrm{Re}\,[\phi(z)] \tag{1}$$

$$p = \int \sigma_{xt}\,\mathrm{d}y - \sigma_{yt}\,\mathrm{d}x = -2\,\mathrm{Im}\,[\mu\phi(z)] \tag{2}$$

$$\sigma_{xt} = 2\,\mathrm{Re}\,[\mu\phi'(z)] \tag{3}$$

$$\sigma_{yt} = 2\,\mathrm{Im}\,[\mu\phi'(z)] \tag{4}$$

where a prime indicates differentiation with respect to the complex variable z. Re and Im stand for the real part and imaginary part, respectively, of a complex function. Before solving this problem with multiple inclusions, we first seek the solution of a single inclusion occupying a region, say S_1, as the form

$$\phi(z) = \phi_0(z) + \underset{\sim}{\phi}(z), \quad z \in S \tag{5}$$

$$\phi^{(1)}(z) = \underset{\sim}{\phi}^{(1)}(z), \quad z \in S_1 \tag{6}$$

where $\phi_0(z)$ represents the solution corresponding to the homogeneous media which is holomorphic in the entire domain except for some singular points. $\underset{\sim}{\phi}(z)$ (or $\underset{\sim}{\phi}^{(1)}(z)$) is the solution associated with the perturbed field of matrix (or inclusion) which is holomorphic in the region S (or S_1). By applying the continuity conditions $u = u_1$ and $p = p_1$, and using the continuation theorem (Muskhelishvili, 1953), one may obtain the following results (Chao and Chiang, 1996)

$$\phi(z) = \phi_0(z) + \alpha_1 \overline{\phi_0(A_1 z)}, \quad z \in S \tag{7}$$

$$\phi^{(1)}(z) = (1+\alpha_1)\phi_0(z), \quad z \in S_1 \tag{8}$$

with

$$\alpha_1 = \frac{\mu - \mu_1}{\mu + \mu_1} \tag{9}$$

where $A_1(z)$ represents the transformation function defined as $A_1 z = a_1^2/(\bar{z} - \bar{z}_1) + z_1$. The overbar denotes the conjugate of a complex function. As to the problem with two circular inclusions, the expressions (7) and (8) are certainly not suitable for this problem since the continuity conditions associated with the second inclusion are not satisfied. Next, we seek the solutions pertaining to the domains S, S_1 and S_2, which are required to satisfy the continuity conditions along the interface L_2 between the second inclusion and matrix. In order to satisfy the interface conditions along the boundary of the second inclusion, the expressions (7) and (8) are now modified to the following expressions:

$$\phi(z) = f_0(z) + \underset{\sim}{f}(z), \quad z \in S \tag{10}$$

$$\phi^{(1)}(z) = (1+\alpha_1)\phi_0(z) + \underset{\sim}{f}(z), \quad z \in S_1 \tag{11}$$

$$\phi^{(2)}(z) = f_0(z) + \underset{\sim}{g}(z), \quad z \in S_2 \tag{12}$$

with

$$f_0(z) = \phi_0(z) + \alpha_1 \overline{\phi_0(A_1 z)} \tag{13}$$

where $\underset{\sim}{f}(z)$ (or $\underset{\sim}{g}(z)$) represents the stress function associated with the perturbed field of matrix (or inclusion) which is holomorphic in the region S (or S_2). Using the continuity conditions of the displacement and resultant force along the interface $z = \sigma = z_2 + a_2 e^{i\theta 2}$, we have the following two equations:

$$\underset{\sim}{f}(\sigma) + \overline{\underset{\sim}{f}(\sigma)} = \underset{\sim}{g}(\sigma) + \overline{\underset{\sim}{g}(\sigma)} \tag{14}$$

$$\mu[f_0(\sigma) + \underset{\sim}{f}(\sigma) - \overline{f_0(\sigma)} - \overline{\underset{\sim}{f}(\sigma)}] = \mu_2[f_0(\sigma) + \underset{\sim}{g}(\sigma) - \overline{f_0(\sigma)} - \overline{\underset{\sim}{g}(\sigma)}] \tag{15}$$

By applying the continuation theorem (Muskhelishvili, 1953), one may define a new set of complex potentials $\theta_j(z)$ $(j = 1, 2)$, which is holomorphic in the entire domain including the interface as

$$\theta_1(z) = \underset{\sim}{f}(z) - \overline{\underset{\sim}{g}(A_2 z)} \tag{16}$$

$$\theta_2(z) = \mu[\underset{\sim}{f}(z) - \overline{f_0(A_2 z)}] + \mu_2[\overline{f_0(A_2 z)} - \overline{\underset{\sim}{g}(A_2 z)}] \tag{17}$$

for $z \in S + S_1$, and

$$\theta_1(z) = \underset{\sim}{g}(z) - \overline{\underset{\sim}{f}(A_2 z)} \tag{18}$$

$$\theta_2(z) = \mu_2[f_0(z) + \underset{\sim}{g}(z)] + \mu[\overline{\underset{\sim}{f}(A_2 z)} - f_0(z)] \tag{19}$$

for $z \in S_2$. $A_2 z$ represents the transformation function defined as $A_2 z = a_2^2/(\bar{z} - \bar{z}_2) + z_2$. Since $\theta_j(z)$ are now holomorphic and single-valued in the whole plane including the point at infinity, by Liouville's theorem we have $\theta_j(z) = \text{const}$. However, the constant functions $\theta_j(z)$ can be treated as a rigid body motion and can thus be assumed to be zero without loss in generality. Based upon this result, (16)–(19) yield the following expressions

$$\underset{\sim}{f}(z) = \alpha_2 \overline{f_0(A_2 z)} \tag{20}$$

$$\underset{\sim}{g}(z) = \alpha_2 f_0(z) \tag{21}$$

with

$$\alpha_2 = \frac{\mu - \mu_2}{\mu + \mu_2} \tag{22}$$

With the help of (20) and (21), the expressions in (10)–(12) become

$$\phi(z) = \phi_0(z) + \alpha_1 \overline{\phi_0(A_1 z)} + \alpha_2 \overline{\phi_0(A_2 z)} + \alpha_2 \alpha_1 \phi_0(A_1 A_2 z) \tag{23}$$

$$\phi^{(1)}(z) = (1 + \alpha_1)\phi_0(z) + \alpha_2 \overline{\phi_0(A_2 z)} + \alpha_2 \alpha_1 \phi_0(A_1 A_2 z) \tag{24}$$

$$\phi^{(2)}(z) = \phi_0(z) + \alpha_1 \overline{\phi_0(A_1 z)} + \alpha_2 \phi_0(z) + \alpha_2 \alpha_1 \overline{\phi_0(A_1 z)} \tag{25}$$

In view of the expressions (23)–(25), the continuity conditions are now satisfied at the interface L_2, but not at the interface L_1. Repeating the previous steps and obtaining the two additional terms each time, the results of which the continuity conditions are satisfied at both the interfaces L_1 and L_2 can be obtained as the following explicit forms

$$\phi(z) = \phi_0(z) + \sum_{n=1}^{\infty} \alpha_{\langle n\rangle}\overline{\phi_{n-1}(A_{\langle n\rangle}z)}, \quad z \in S \tag{26}$$

$$\phi^{(1)}(z) = \phi_0(z) + \sum_{n=0}^{\infty} \{\alpha_1\phi_{2n}(z) + \alpha_2\overline{\phi_{2n+1}(A_2 z)}\}, \quad z \in S_1 \tag{27}$$

$$\phi^{(2)}(z) = \phi_1(z) + \sum_{n=0}^{\infty} \{\alpha_2\phi_{2n+1}(z) + \alpha_1\overline{\phi_{2n+2}(A_1 z)}\}, \quad z \in S_2 \tag{28}$$

with

$$\phi_1(z) = \phi_0(z) + \alpha_1\overline{\phi_0(A_1 z)} \tag{29}$$

$$\phi_n(z) = \alpha_{\langle n\rangle}\overline{\phi_{n-1}(A_{\langle n\rangle}z)}, \quad n \geqslant 2 \tag{30}$$

where $\langle n\rangle = 1$ for $n = 1, 3, 5, 7, 9, \ldots$, etc., and $\langle n\rangle = 2$ for $n = 2, 4, 6, 8, 10, \ldots$, etc. The expressions given by (26)–(28) are exactly the same as those obtained by Honein *et al.* (1992b) who employed the methodology of "heterogenization" and the structure of Moebius transformations. Based upon the method of successive approximations described earlier, the solutions, similar to the expressions (26)–(28) obtained for two circular inclusions, can be extended to the problem containing any number of circular inclusions ($m \geqslant 2$) as the following elegant forms

$$\phi(z) = \phi_0(z) + \sum_{n=1}^{\infty} \alpha_{\langle n\rangle}\overline{\phi_{n-1}(A_{\langle n\rangle}z)}, \quad z \in S \tag{31}$$

$$\phi^{(j)}(z) = \phi_{j-1}(z) + \sum_{n=0}^{\infty} \{\alpha_j\phi_{m\times n+j-1}(z) + \sum_{i=1}^{m-1} \alpha_{\langle i+j\rangle}\overline{\phi_{m\times n+i+j-1}(A_{\langle i+j\rangle}z)}\},$$

$$z \in S_j \quad (1 \leqslant j \leqslant m) \tag{32}$$

with

$$\phi_l(z) = \phi_{l-1}(z) + \alpha_{\langle l\rangle}\overline{\phi_{l-1}(A_{\langle l\rangle}z)}, \quad 1 \leqslant l < m-1 \tag{33}$$

$$\phi_l(z) = \sum_{k=0}^{m-2} \alpha_{\langle l-k\rangle}\overline{\phi_{l-k-1}(A_{\langle l-k\rangle}z)}, \quad l \geqslant m \tag{34}$$

where m is the number of circular inclusions and the symbol $\langle n\rangle$ is defined as

$$\langle n\rangle = \mathrm{REM}\{(n-1)/m\} + 1 \tag{35}$$

Here the function $\mathrm{REM}\{(n-1)/m\}$ represents the remainder of the fraction $(n-1)/m$. For example, when $m = 3$, $\mathrm{REM}\{(n-1)/3\} = 0$, for $n = 1, 4, 7, 10$, etc., $\mathrm{REM}\{(n-1)/3\} = 1$, for $n = 2, 5, 8, 11$, etc., and $\mathrm{REM}\{(n-1)/3\} = 2$, for $n = 3, 6, 9, 12$, etc. From the definition (35), it is understood that $\langle n\rangle \leqslant m$. The parameter α_j and the transformation function $A_j z$ appearing in (31) and (32) stand for

$$\alpha_j = \frac{\mu - \mu_j}{\mu + \mu_j} \tag{36}$$

and

$$A_j z = \frac{a_j^2}{(\bar{z} - \bar{z}_j)} + z_j \tag{37}$$

corresponding to the j-th circular inclusion. It is worthy to note that the present derived solutions can also be applied to the inclusion problem with straight boundaries if one replaces (37) by

$$A_j z = \bar{z} + 2ih_j \tag{38}$$

for the corresponding multiple layer problem with the depth h_j associated with the j-th material layer. Equations (31) and (32) give the general series solutions to the antiplane problem containing an arbitrary array of m circular inclusions provided that the corresponding homogeneous solution $\phi_0(z)$ is appropriately solved. Note that the series solutions in (31) and (32) are uniformly convergent on compact sets provided $|\alpha_j| < 1$. The case $\alpha_j = 1$ corresponds to a circular hole while $\alpha_j = -1$ corresponds to a rigid inclusion. In all other cases $|\alpha_j| < 1$ as expected from (36). Even for the case of $\alpha_j = 1$ or $\alpha_j = -1$, the convergent series solutions representing the derivative of the complex potentials of the stress field can also be achieved if one differentiates the formal series solutions (31) and (32) term by term (Honein *et al.*, 1992b).

3. CRACK INTERACTION WITH INCLUSIONS

In this section, we consider a single crack embedded in the matrix under remote uniform load (Fig. 2). The current problem can be treated as a sum of the corresponding multiple inclusion problem without cracks and a corrective problem. The solution related to the former problem an be directly obtained from (31) with $\phi_0(z)$ being

$$\phi_0(z) = \tau_{\infty} z \tag{39}$$

where τ_{∞} is the magnitude of remote uniform load applied along the x-direction. On the other hand, a corrective solution associated with a single crack L can be obtained by substituting

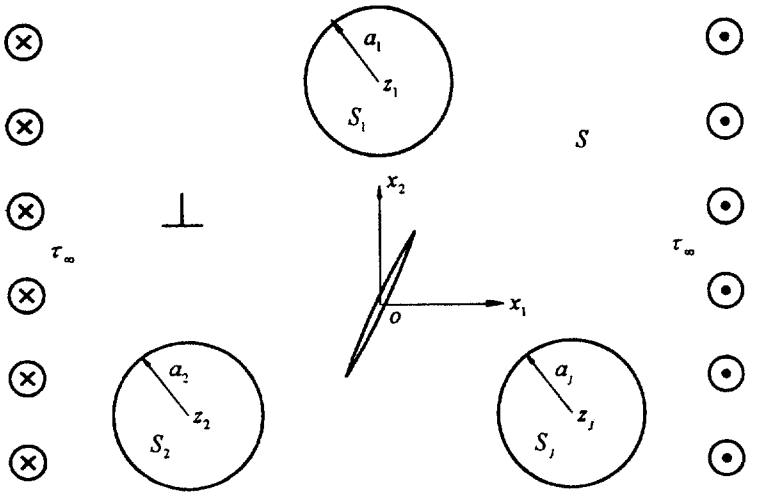

Fig. 2. A single crack interacted with multiple circular inclusions.

$$\phi_0(z) = -\frac{i}{2\pi}\int_L b_0(t)\log(z-t)\,dt \tag{40}$$

into (31). The unknown function $b_0(t)$ in (40) can be determined in the sense that the traction free acting on the crack surface associated with a corrective problem must be balanced by the given traction force $p^{(u)}$ resulted from the corresponding unflawed problem, i.e.

$$p^{(w)}(z) = -2\,\mathrm{Im}\,[\mu\phi(t)] + c_0, \quad t \in L \tag{41}$$

where c_0 is an additive constant to be determined. In addition, the single-valued condition when enclosing the crack surface must be satisfied, i.e.

$$\int_L b_0(t)\,dt = 0 \tag{42}$$

Substituting of (40) into (31) and applying (41) yield the singular integral equation together with the subsidiary condition, (42), which may be solved numerically. To perform the numerical calculations, the following interpolation formulae in local coordinates s_j $(1 \leqslant j \leqslant N)$ (see Fig. 3) are introduced as (Chen, 1990)

$$b_0(t_1) = b_{0,0}\left(\sqrt{\frac{2d_1}{t_1}} - 1\right) + b_{0,1} \tag{43}$$

$$b_0(t_N) = b_{0,N}\left(\sqrt{\frac{2d_N}{2d_N - t_N}} - 1\right) + b_{0,N-1} \tag{44}$$

and

$$b_0(t_j) = b_{0,j-1}\frac{2d_j - t_j}{2d_j} + b_{0,j}\frac{t_j}{2d_j}, \quad (2 \leqslant j \leqslant N-1) \tag{45}$$

where d_j $(1 \leqslant j \leqslant N)$ are the half length of each line segment and $b_{0,j}$ $(0 \leqslant j \leqslant N)$ are the

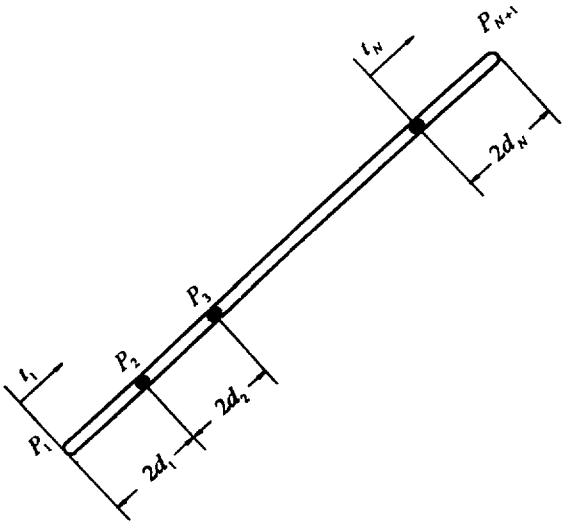

Fig. 3. Division and nodal distribution of a straight crack.

unknown coefficients which can be determined numerically (Chen, 1990; Chao and Shen, 1995). Once the coefficients $b_{0,j}$ are determined, the mode-III stress intensity factors can be obtained accordingly as (Chen, 1990)

$$K_{\mathrm{III}}(\mathrm{tip}-A) = \pi(2\pi)^{1/2} \lim_{t_1 \to 0} b_0(t_1) t_1^{1/2} = 2\pi\sqrt{\pi d_1}\, b_{0,0} \tag{46}$$

$$K_{\mathrm{III}}(\mathrm{tip}-B) = \pi(2\pi)^{1/2} \lim_{t_N \to 2d_N} b_0(t_N)(2d_N - t_N)^{1/2} = 2\pi\sqrt{\pi d_N}\, b_{0,N} \tag{47}$$

4. EXAMPLES

The fundamental series solution derived in the preceding sections will be used to analyze the following examples associated with three circular inclusions embedded in an infinite matrix and in a half-plane matrix, and in a strip.

(a) *Elastic inclusions under remote uniform load*

As our first example, we consider three circular inclusions perfectly bonded to a matrix which is subjected to uniform load τ_∞ at infinity along the x-axis (see Fig. 4). The solution of the corresponding homogeneous problem is trivially given as (39). The stress field associated with the heterogeneous problem can be immediately obtained from (31) and (32) with the aid of (3) and (4). In order to demonstrate the accuracy and usefulness of the present proposed method, the stress concentration of the problem with two equal-sized holes, which is determined by summing up the first thirty terms in (31), is illustrated in Fig. 5. It is shown that the present results agree very well with those obtained by Steif (1989) even the case when the two holes approach each other. In the following examples, we only focus on the local stress along a circular hole surrounded by two elastic circular inclusions with equal radius $a_1 = a_2$, and equal shear modulus $\mu_1 = \mu_2$. Figures 6–9 display the distribution of the tangential stress along a circular hole influenced by the surrounding elastic solutions. All the calculated results shown in Figs 6–9 are determined by summing up the first forty terms in (31) which have been checked to achieve a good accuracy with an error less than 0.1% as compared to a sum of the first sixty terms in (31). The stress distribution along a circular hole affected by the presence of two surrounding elastic inclusions, when they are arrayed parallel or perpendicular to the direction of remote load, is shown in Figs

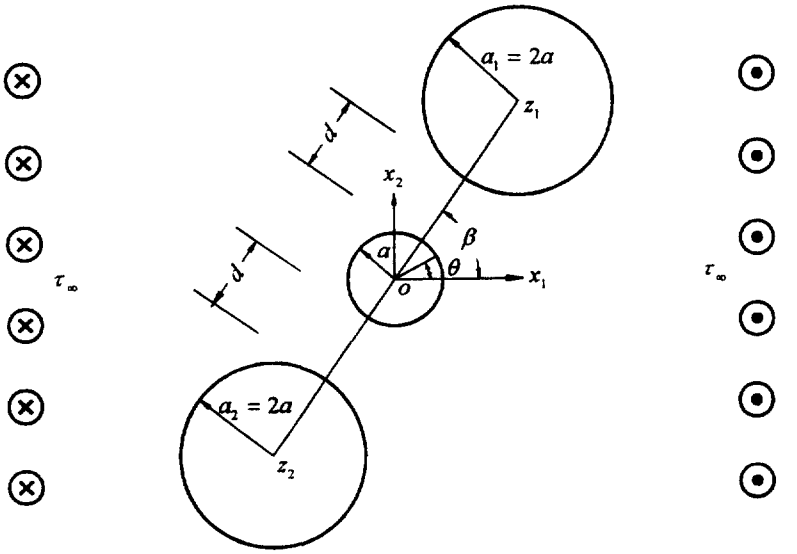

Fig. 4. A circular hole surrounded by two circular elastic inclusions under a remote uniform load along the x-axis.

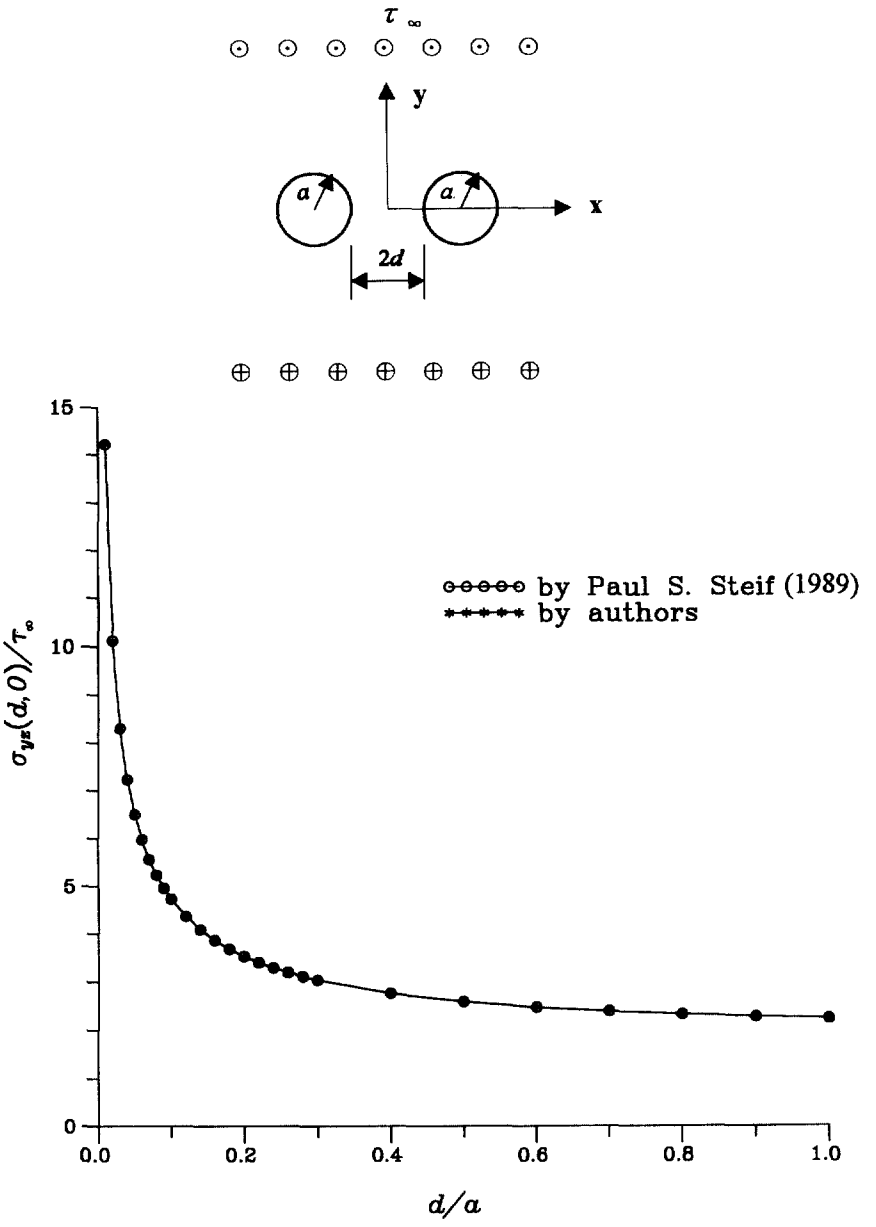

Fig. 5. Stress concentration of the problem with two equal-sized holes.

6–7. It is seen that the tangential shear stress along a hole is intensified or diminished depending on the shear strength of inclusions and the relative location between the applied load and the inclusions. Some interesting results show that, when a hole and two inclusions are arrayed parallel to the applied load, i.e., $\beta = 0^\circ$ (see Figs 6 and 8), the stress concentration factor τ_θ/τ_∞, reached at $\theta = 90^\circ$, along a circular hole increases (or decreases) as the neighboring hard (or soft) inclusions approach a circular hole. On the contrary, when a hole and two inclusions are arrayed perpendicular to the applied load, i.e., $\beta = 90^\circ$ (see Figs 7 and 9), the stress concentration factor, reached at $\theta = 90^\circ$, decreases (or increases) as the neighboring hard (or soft) inclusions approach a circular hole. It is worthy to note that the present derived solution is still valid for the case when two circular inclusions touch each other. It is found that the stress at the point of contact between a hole and the neighboring elastic inclusions remains finite for any orientation of remote load while the contact stress between two neighboring holes becomes unbounded for any orientation of

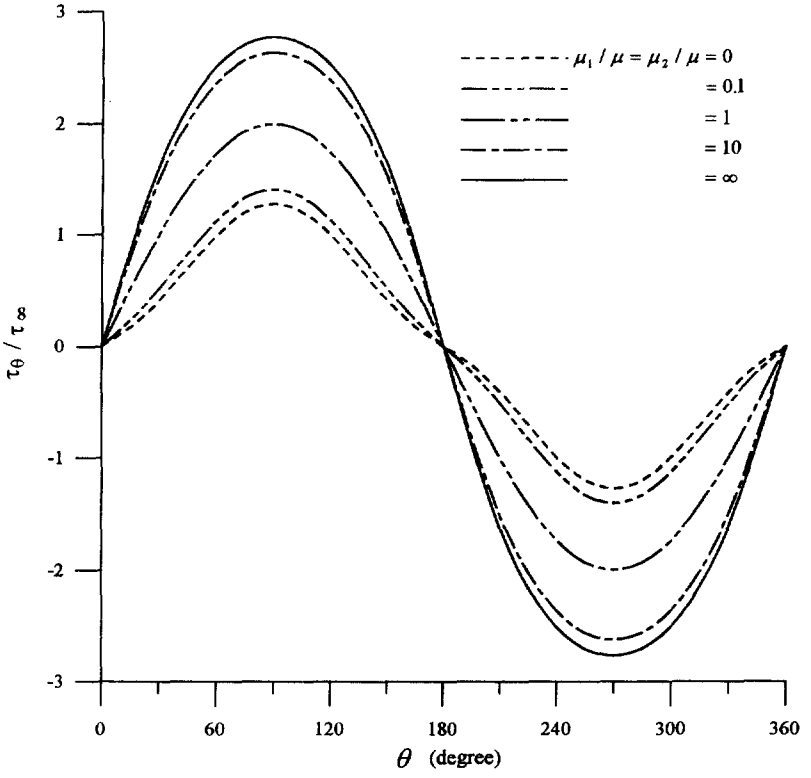

Fig. 6. Tangential stress distribution along the hole boundary with $\beta = 0°$.

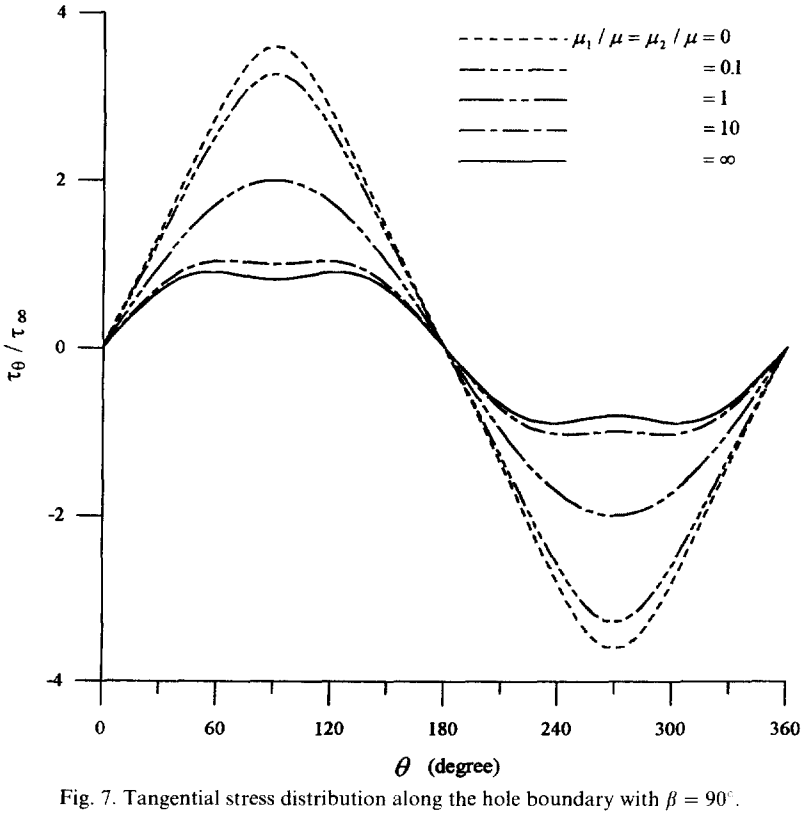

Fig. 7. Tangential stress distribution along the hole boundary with $\beta = 90°$.

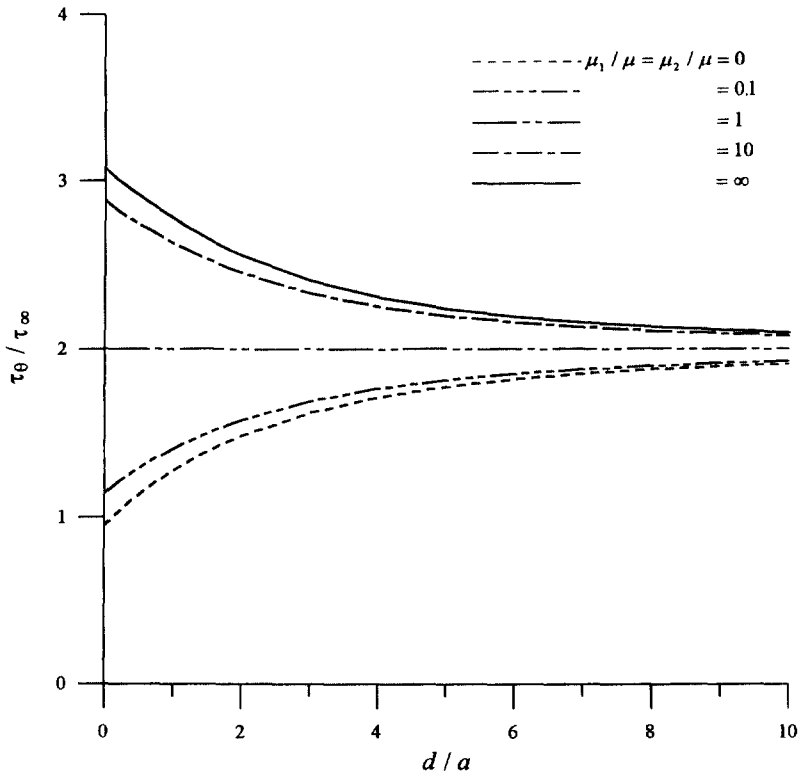

Fig. 8. Stress concentration as a function of the spacing d/a with $\beta = 0^\circ$.

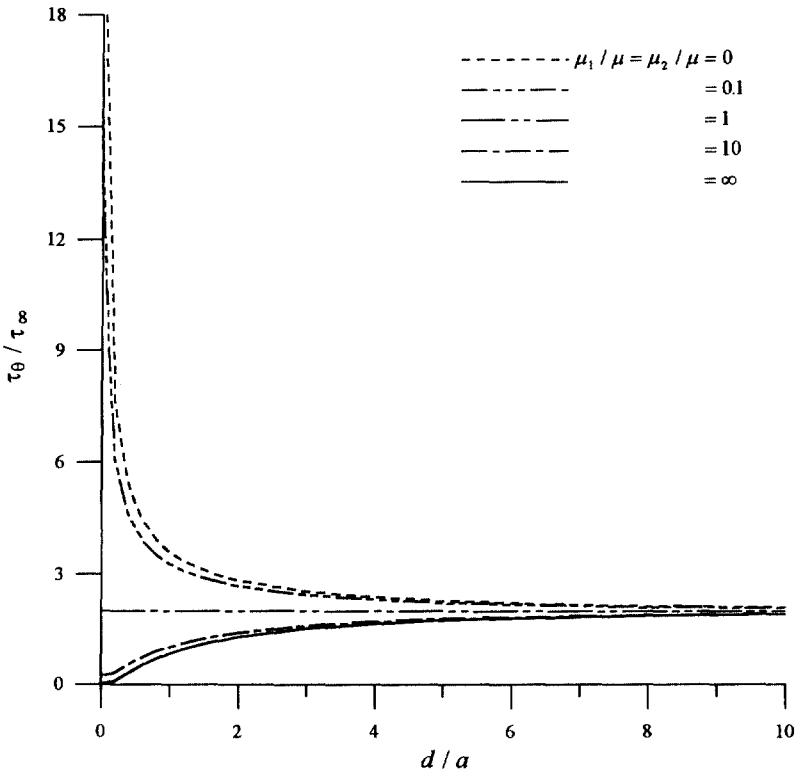

Fig. 9. Stress concentration as a function of the spacing d/a with $\beta = 90^\circ$.

remote load except for the case when a line joining the centers of the three holes is parallel to the applied load.

(b) *Point force acting on the half-plane surface*

As a second example we consider a hole and two circular inclusions embedded in a half-plane matrix which is subjected to a point force p_0 acting at its surface $z = ih$ (see Fig. 10). The solution associated with the corresponding half-plane problem can be immediately obtained by substituting $A_4 z = \bar{z} + 2ih$ and $\alpha_4 = 1$ into (31) with $\phi_0(z)$ being

$$\phi_0(z) = p_0 \lim_{y \to h} \log(z - iy) \tag{48}$$

Figures 11–13 exhibit the variation of the local stress along a circular hole influenced by

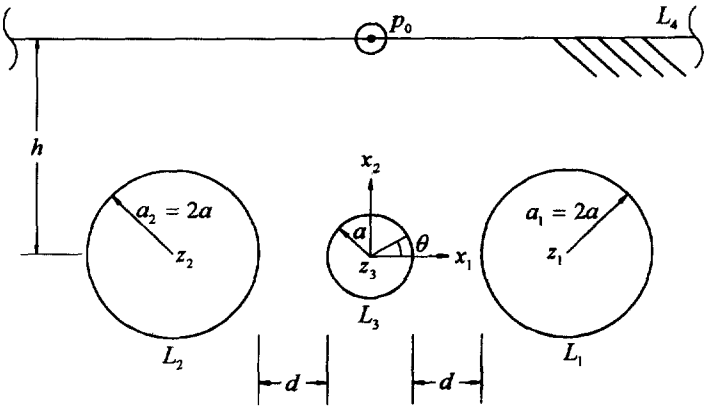

Fig. 10. A circular hole and two circular inclusions perfectly bonded to a half-plane matrix.

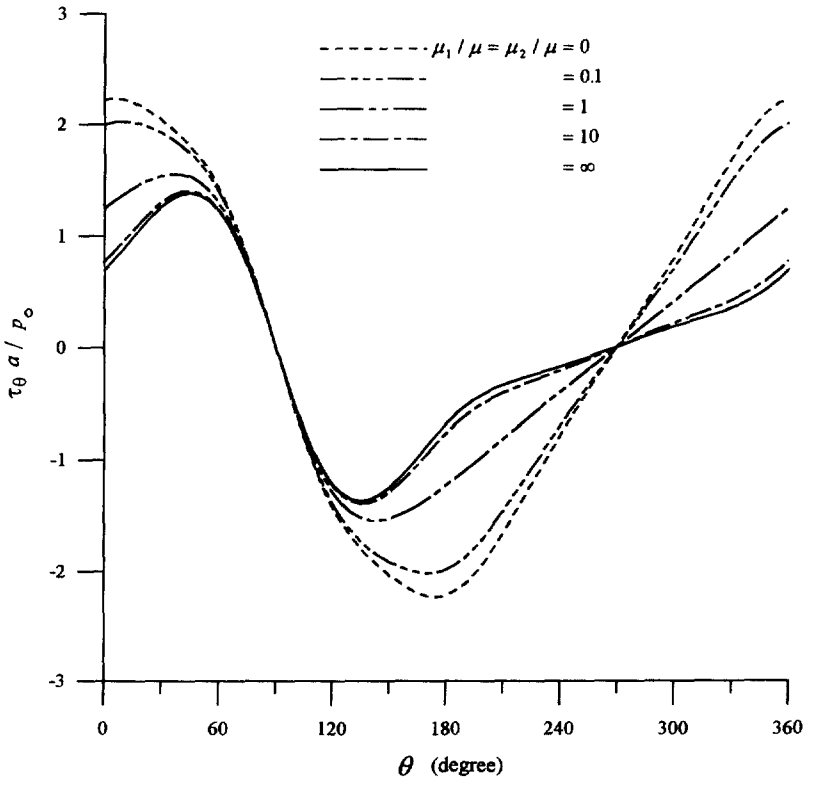

Fig. 11. Tangential stress distribution for different ratios of shear modulus with $d/a = 1$ and $h/a = 3$.

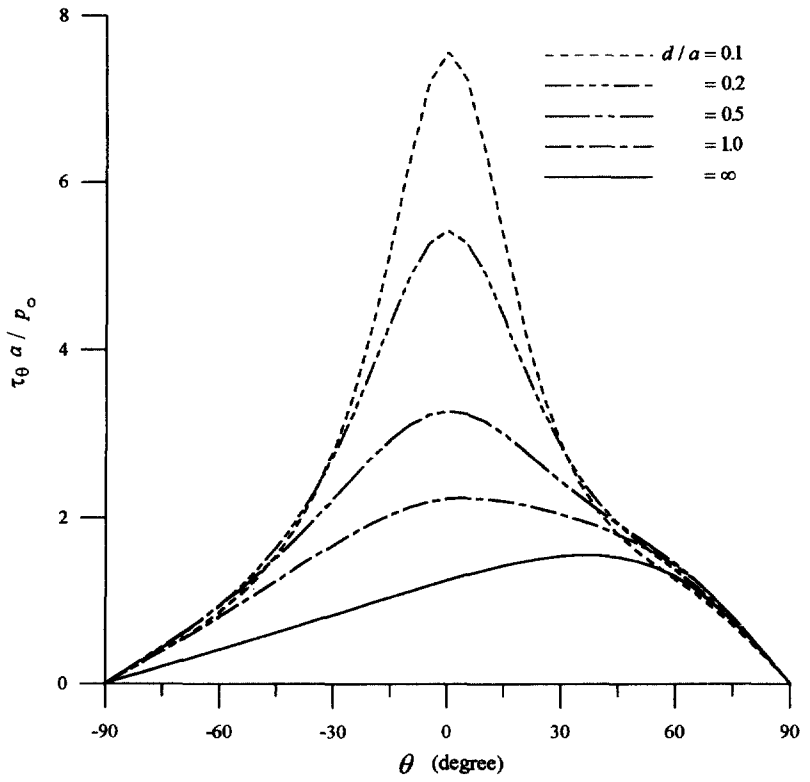

Fig. 12. Tangential stress distribution influenced by two surrounding circular holes with $h/a = 3$.

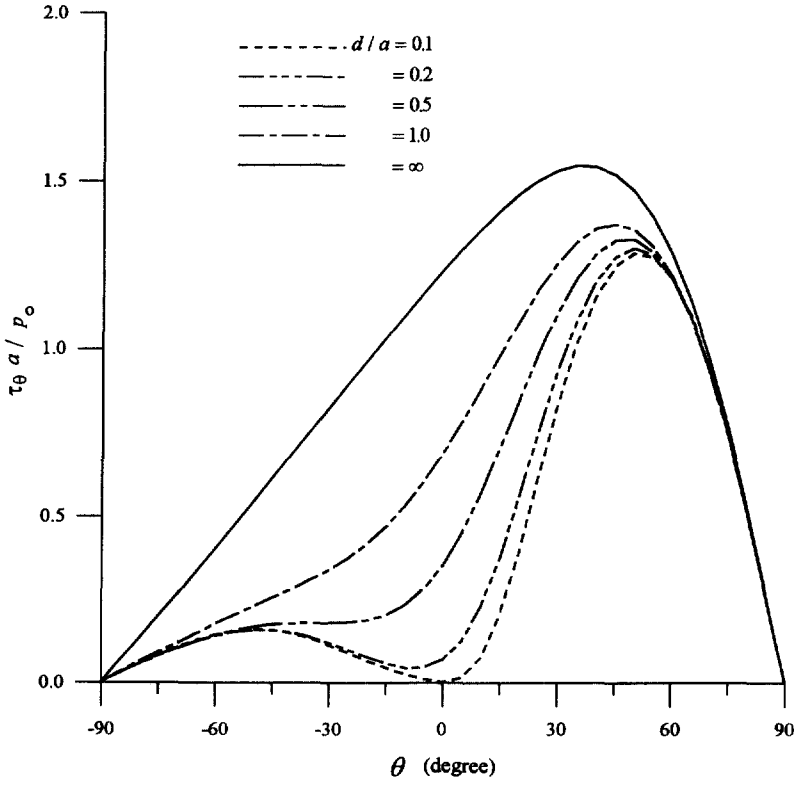

Fig. 13. Tangential stress distribution influenced by two surrounding rigid inclusions with $h/a = 3$.

the surrounding circular inclusions. All the calculated results displayed in Figs 11–13 are obtained from the series solution up to the first 192 terms in (31) which are checked to gain a good accuracy. Let the distance between the circular hole and the neighboring inclusions be $d/a = 1$ and the distance between the circular hole and the free surface of half-plane be $h/a = 3$. The maximum stress along the boundary of the circular hole occurs at the angle θ between 0 and 45° (or between 135 and 180°) depending on the shear modulus of the surrounding inclusions (see Fig. 11). In fact, there are three parameters, namely, the relative angle φ, the distance ρ, and the ratio μ_1/μ (or μ_2/μ) affecting the local stress along a circular hole. The relative angle φ is defined as the angle between a line tangent to the point of interest along a hole and a line connecting the point of interest and the applied load. The parameter ρ is defined as the distance between the point of interest along a hole and the applied load. In general, the stress along a circular hole increases with decreasing of the distance ρ while decreases with increasing of the angle φ. Precisely, the tangential stress along a hole would vanish at $\varphi = 90°$ (or $\theta = 90, 270°$ in the present case) even though the distance ρ is infinitely close to zero. Increasing or decreasing of the tangential stress would compete depending on the relative angle φ and the distance ρ. The stress concentration along a circular hole can be further intensified (or diminished) by the surrounding inclusions having a lower (or higher) shear modulus as discussed in example (a). Strong interaction between a hole and two neighboring holes (or two neighboring rigid inclusions) is observed if the distance d/a between them decreases as indicated in Figs 12–13. It is found that the maximum tangential stress may occur along a hole near the point $\theta = 0°$ as the two neighboring holes approach each other while near the point $\theta = 45°$ as the two neighboring rigid inclusions approach a hole. This is simply because the stress would dramatically increase at the point along a circular hole which is nearest to the neighboring holes. On the other hand, the stress may decrease at the point along a circular hole which is nearest to the neighboring rigid inclusions.

(c) *Point forces acting on the surfaces of a strip*

As our third example we consider a hole and two circular inclusions embedded in a strip with thickness $2h$ which is subjected to a pair of equal and opposite concentrated force at its surfaces (see Fig. 14). The corresponding homogeneous solution can be obtained by adding the function $\phi_0(z)$ being (48) associated with the point force p_0 acting at $z = ih$ and the function $\theta_0(z)$ being

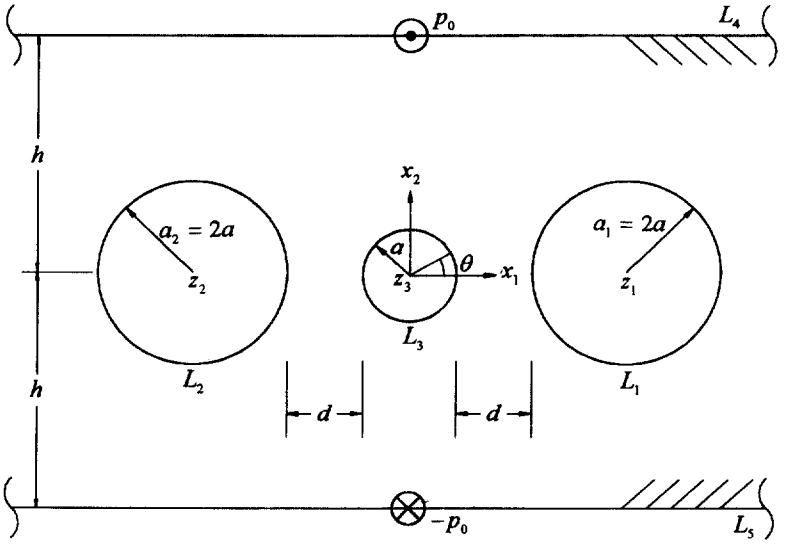

Fig. 14. A circular hole and two circular inclusions embedded in an infinite strip with thickness $2h$.

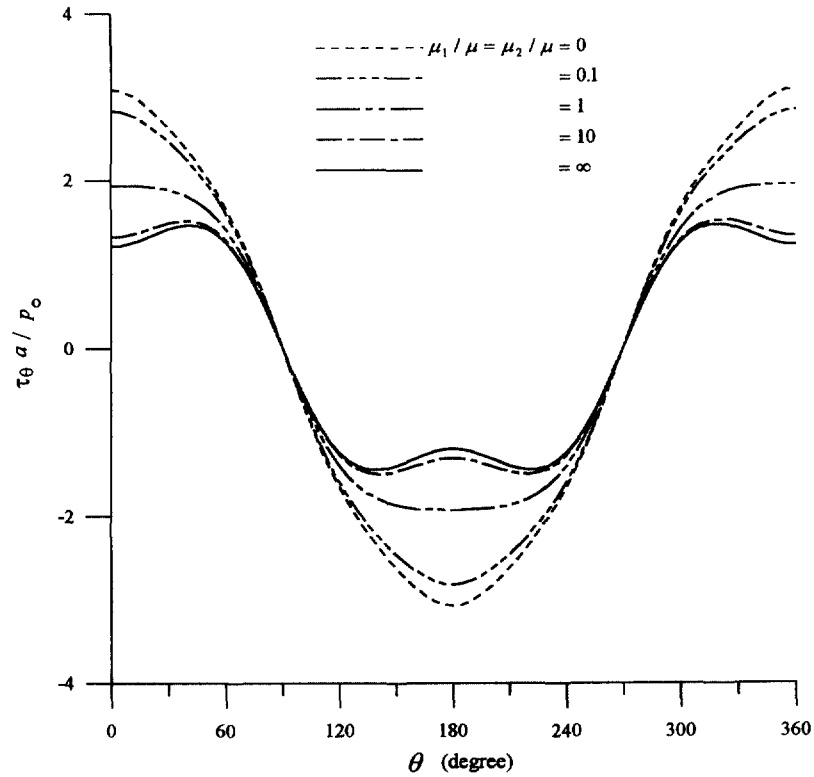

Fig. 15. Tangential stress distribution for different ratios of shear modulus with $d/a = 1$ and $h/a = 3$.

$$\phi_0(z) = -p_0 \lim_{y \to h} \log(z + iy) \tag{49}$$

associated with the point force $-p_0$ acting at $z = -ih$. The solution associated with the corresponding strip problem may be directly determined from (31) and (32) if one chooses $A_4 z = \bar{z} + 2ih$, $A_5 z = \bar{z} - 2ih$, and $\alpha_4 = \alpha_5 = 1$. All the calculated results displayed in Figs 15–17 are based on the series solution up to the first 752 terms in (31) which are checked to preserve a good accuracy. Figure 15 displays the tangential stress distribution along a hole which is away from the surrounding elastic inclusions and the free surfaces of a strip with the distance $d/a = 1$ and $h/a = 3$, respectively. The maximum tangential stress occurs at the point $\theta = 0°$ if the neighboring inclusions are made less rigid than the matrix and at the point near $\theta = 45°$ if the neighboring inclusions are made more rigid than the matrix. Figures 16–17 show the local stress distribution along a hole as the neighboring rigid inclusions (or holes) approach each other. The results indicate that, similar to the conclusions of the preceding examples, the maximum stress concentration, which occurs at the point on the boundary of the hole which is nearest to the neighboring holes, becomes unbounded as the distance between the hole and two surrounding holes decreases. On the other hand, the maximum stress concentration, which occurs at the point around $\theta = 50°$ (or $\theta = -50°$) on the boundary of the hole, remains bounded as the two surroundings rigid inclusions approach the hole.

(d) *Elastic solutions interacted with a crack*

As a fourth example we consider a single crack interacted with three circular inclusions with equal radius $a_1 = a_2 = a_3$ and equal shear modulus $\mu_1 = \mu_2 = \mu_3$ embedded in an infinite matrix (see Fig. 18). In order to demonstrate the accuracy of the present crack problem, we now consider an infinite body containing a pair of circular holes spaced apart by a distance $2d$ and a crack of length $2a$ located symmetrically on the line connecting the centers of the two holes (see Fig. 19). The calculated stress intensity factors as displayed in

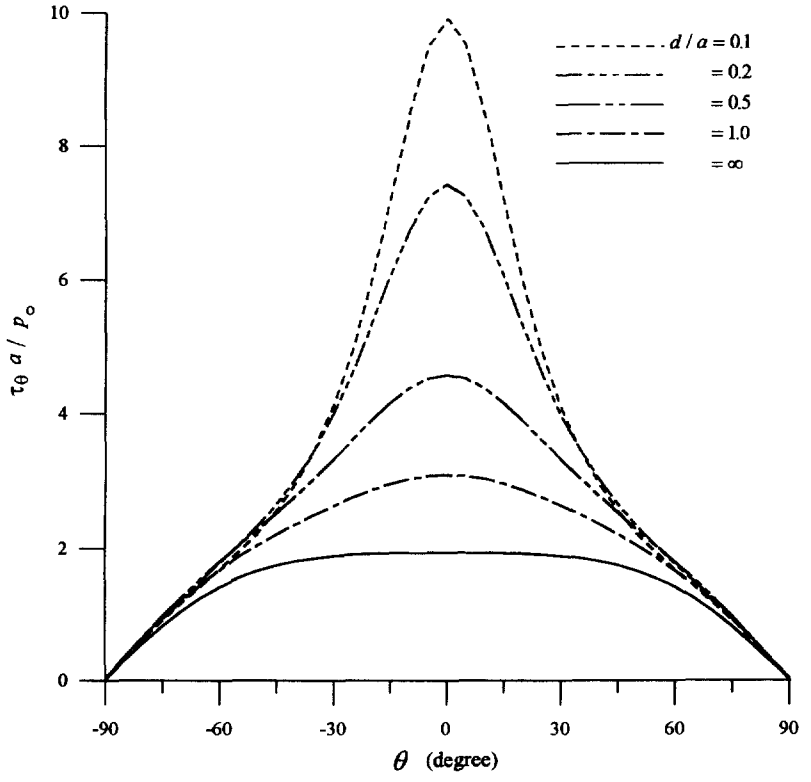

Fig. 16. Tangential stress distribution influenced by two surrounding circular holes with $h/a = 3$.

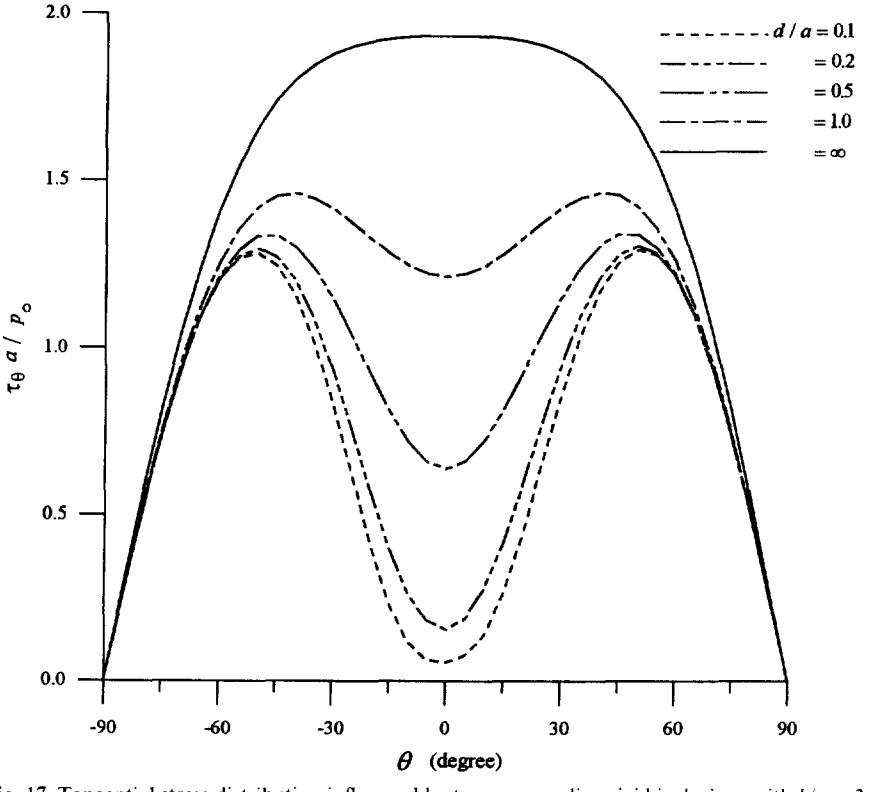

Fig. 17. Tangential stress distribution influenced by two surrounding rigid inclusions with $h/a = 3$.

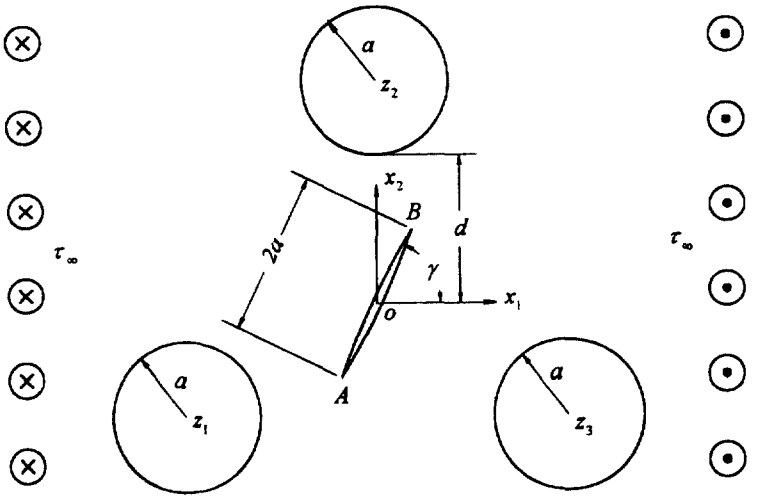

Fig. 18. A single crack surrounded by the three surrounding elastic inclusions with equal spacing d/a.

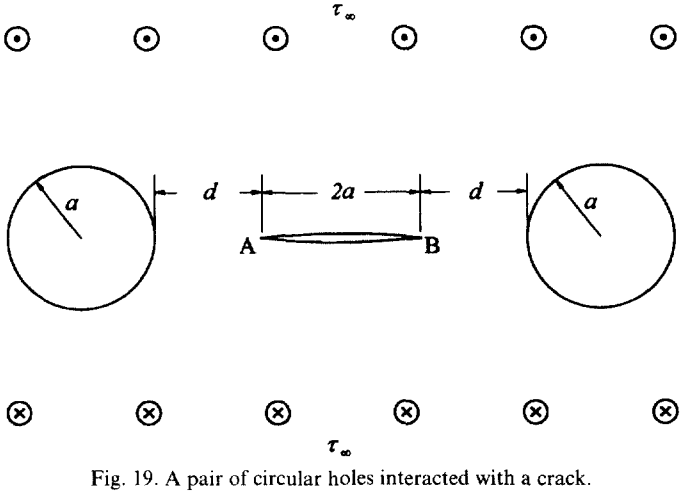

Fig. 19. A pair of circular holes interacted with a crack.

Fig. 20, which are obtained from (46) with the number of line segment $N = 50$, are shown to agree very well with those provided by Isida (1973). Figures 21 and 22 exhibit the variation of stress intensity factors with the crack angle β where a crack is surrounded by the three circular elastic inclusions with the spacing $d/a = 3$. It is found that the stress intensity factor at tip-A increases with decreasing the ratio μ_1/μ for the crack angle ranging from $-90°$—$-48°$ and from $42°$–$90°$ while decreases with decreasing the ratio μ_1/μ for the crack angle ranging from $-48°$–$42°$. This is because the presence of elastic inclusions may act as a shield or an anti-shield depending on the relative location between the applied load and the inclusions as discussed in the preceeding examples. Same arguments can also be applied to the case for tip-B as seen in Fig. 22. The stress intensity factors at both tip-A and tip-B are plotted in Figs 23 and 24, respectively, as a function of the spacing d/a with the crack angle $\beta = 90°$. It is shown that the stress intensity factor at tip-A (or tip-B) tends to monotonically decrease (or increase) as the surrounding holes ($\mu_1/\mu = 0$) approach a crack while the stress intensity factor at tip-A (or tip-B) becomes to monotonically increase (or decrease) as the surrounding rigid inclusions ($\mu_1/\mu = \infty$) approach a crack. As a limiting case of $d/a \gg 1$, the dimensionless stress intensity factors approach one which coincides with the result of the corresponding homogeneous problem containing a central crack.

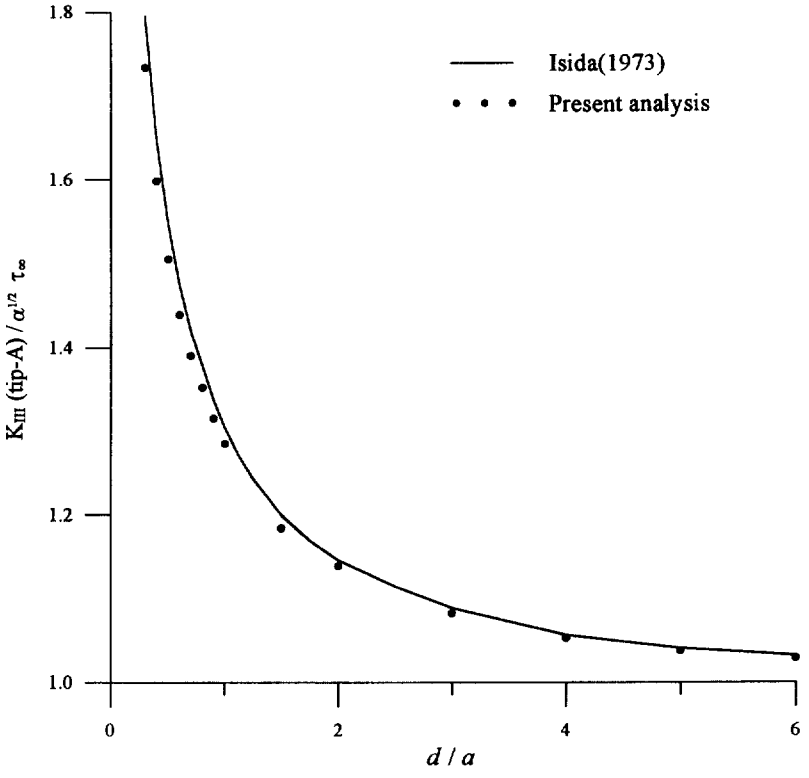

Fig. 20. Stress intensity factor as a function of the spacing d/a.

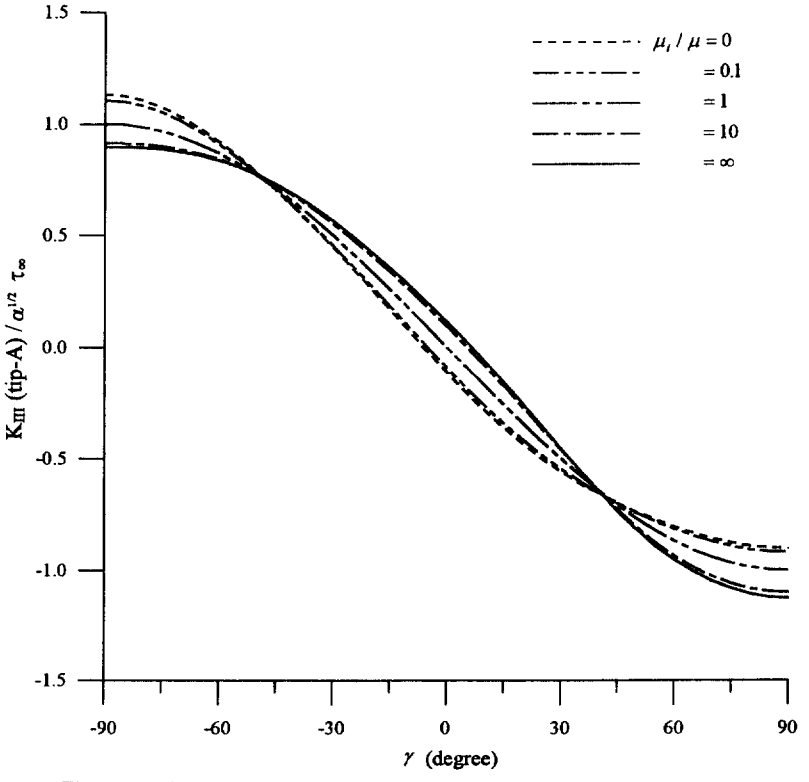

Fig. 21. Variations of stress intensity factor at tip-A with the crack angle γ.

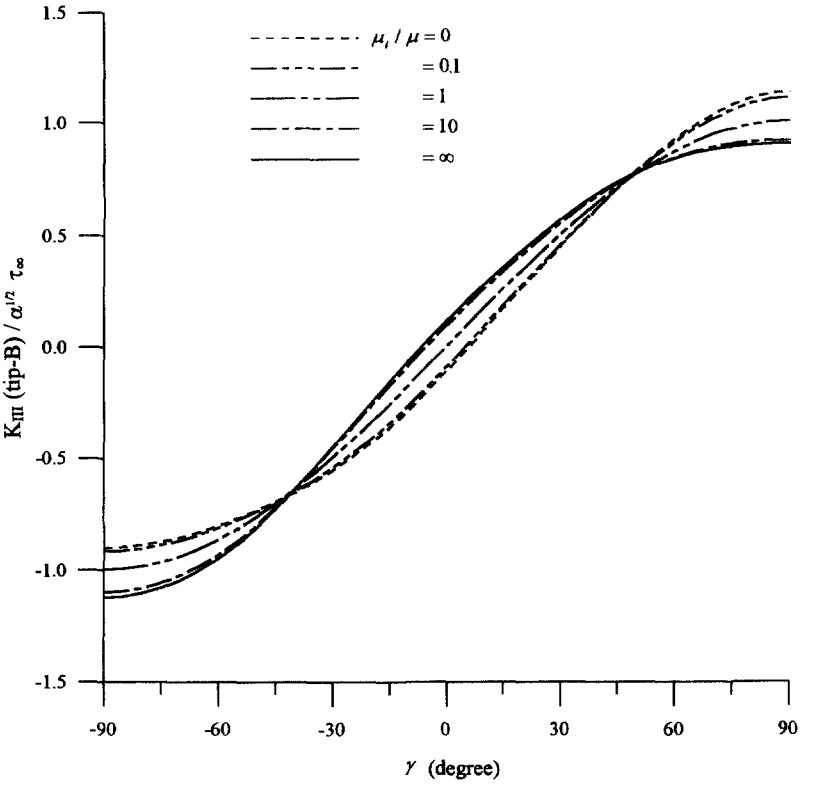

Fig. 22. Variations of stress intensity factor at tip-B with the crack angle γ.

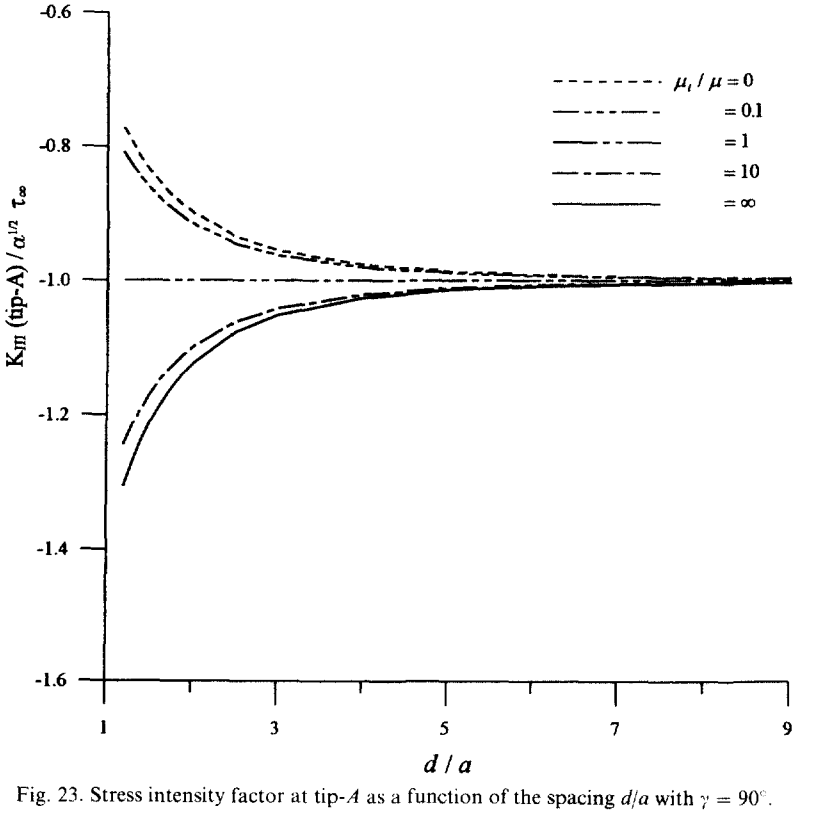

Fig. 23. Stress intensity factor at tip-A as a function of the spacing d/a with $\gamma = 90°$.

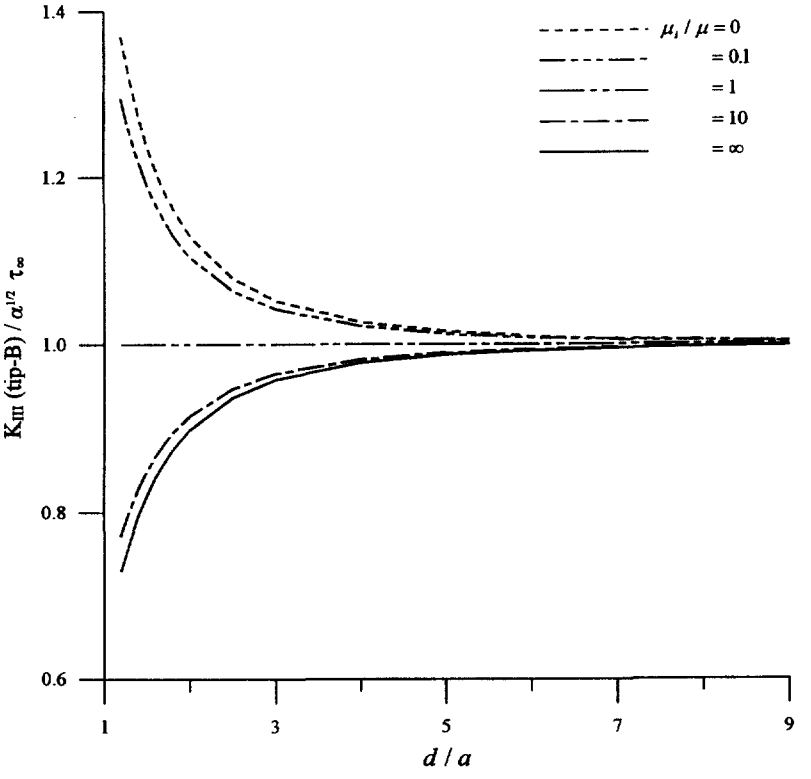

Fig. 24. Stress intensity factor at tip-B as a function of the spacing d/a with $\gamma = 0^{\circ}$.

5. CONCLUDING REMARKS

The antiplane problem of multiple circular inclusions of different radii and of different shear moduli, perfectly bonded to a matrix of infinite extent, is analyzed in this paper. Within the framework of the procedure of analytical continuation and the method of successive approximations, the solution associated with the heterogeneous problem is sought as a transformation on the solution to the corresponding homogeneous problem. Due to this important property, the solution related to the problem containing any number of inclusions can be immediately obtained as the corresponding homogeneous solution is solved. Numerical examples of three circular inclusions embedded in an infinite matrix, in a half-plane matrix, and in an infinite strip are used to demonstrate the efficiency and universality of the present approach. The stress intensity factor of a single crack interacted with the surrounding circular inclusions is also examined and discussed in the present study.

REFERENCES

Chao, C. K. and Chiang, T. F. (1996) Antiplane interaction of an anisotropic elliptic inclusion with an arbitrarily oriented crack. *International Journal of Fracture* **75,** 229–245.

Chao, C. K. and Shen, M. H. (1995) Solution of thermoelastic crack problems in bonded dissimilar media or half-plane medium. *International Journal of Solids and Structures* **32,** 3537–3554.

Chao, C. K., Shen, M. H and Fung, C. K. (1997) On multiple circular inclusions in plane thermoelasticity. *International Journal of Solids and Structures* **34,** 1873–1892.

Chen, Y. Z. (1990) New integral equation for curve crack problem in plane elasticity with arbitrary loading condition. *International Journal of Fracture* **46,** R43–R46.

Goree, J. G. and Wilson, Jr, H. B. (1967) Transverse shear loading in an elastic matrix containing two circular cylindrical inclusions. *Journal of Applied Mechanics* **34,** 511–513.

Gong, S. X. (1995) Antiplane interaction among multiple circular inclusions. *Mech. Rech. Communications* **22,** 257–262.

Honein, E., Honein, T. and Herrmann, G. (1992a) Further aspects of the elastic field for two circular inclusions in antiplane elastostatics. *Journal of Applied Mechanics* **59,** 774–779.

Honein, E., Honein, T. and Herrmann, G. (1992b) On two circular inclusions in harmonic problems. *Quarterly of Applied Mathematics* **L3,** 479–499.

Horii, H. and Nemat-Nasser, S. (1985) Elastic fields of interacting inhomogeneities. *International Journal of Solids and Structures* **21,** 731–745.

Isida, M. (1973) *Methods of Analysis and Solutions of Crack Problems*, ed. G. C. Sih. Noordhoff, Groningen.

Kienzler, R. and Duan Zhuping (1987) On the distribution of hoop stresses around circular holes in elastic sheets. *Journal of Applied Mechanics* **54,** 110–114.

Muskhelishvili, N. I. (1953) Some basic problems of the mathematical theory of elasticity. Noordhoff, Groningen.

Noda, N. A. and Matsuo, T. (1997) Numerical solution of singular integral equations in stress concentration problems. *International Journal of Solids and Structures* **34,** 2429–2444.

Sendeckyj, G. P. (1971) Multiple circular inclusion problems in longitudinal shear deformation. *Journal of Elasticity* **1,** 83–86.

Steif, Paul S. (1989) Shear stress concentration between holes. *Journal of Applied Mechanics*, **56,** 719–721.

Zimmerman, R. W. (1988) Stress concentration around a pair of circular holes in a hydrostatically stressed elastic sheet. *Journal of Applied Mechanics* **55,** 487–488.